Recent 121-year variability of western boundary upwelling in the northern South China Sea

Yi Liu,[1,2] Zicheng Peng,[1] Chuan-Chou Shen,[3] Renjun Zhou,[4] Shaohua Song,[2] Zhengguo Shi,[2] Tegu Chen,[5] Gangjian Wei,[6] and Kristine L. DeLong[7]

Received 12 March 2013; accepted 18 March 2013; published 18 June 2013.

[1] Coastal upwelling is typically related to the eastern boundary upwelling system, whereas the powerful southwest Asian summer monsoon can also generate significant cold, nutrient-rich deep water in western coastal zones. Here we present a sea surface temperature record (A.D. 1876–1996) derived from coral *Porites* Sr/Ca for an upwelling zone in the northern South China Sea. The upwelling-induced sea surface temperature anomaly record reveals prominent multidecadal variability driven by Asian summer monsoon dynamics with an abrupt transition from warmer to colder conditions in 1930, and a return to warmer conditions after 1960. Previous studies suggest the expected increase in atmospheric CO_2 for the coming decades may result in intensification in the eastern boundary upwelling system, which could enhance upwelling of CO_2-rich deep water thus exacerbating the impact of acidification in these productive zones. In contrast, the weakening trend since 1961 in the upwelling time series from the northern South China Sea suggests moderate regional ocean acidification from upwelling thus a stress relief for marine life in this region. **Citation:** Liu, Y., Z. Peng, C.-C. Shen, R. Zhou, S. Song, Z. Shi, T. Chen, G. Wei, and K. L. DeLong (2013), Recent 121-year variability of western boundary upwelling in the northern South China Sea, *Geophys. Res. Lett.*, *40*, 3180–3183, doi:10.1002/grl.50381.

1. Introduction

[2] Globally, seafood provides 11% of the animal protein source for human beings [*Food and Agriculture Organization*, 2011] with 50% of this protein supplied from coastal upwelling regions [*Summerhayes*, 1996]. Understanding the behavior of coastal upwelling in the face of global climate change is a challenge because upwelling in the preinstrumental period is poorly documented [*McGregor et al.*, 2007] and climate models have difficulties providing consistent upwelling results [*Wang et al.*, 2010]. It has become increasingly important to understand these regions for the coming decades due to the possible dramatic ecosystem and socioeconomic impacts [*Bakun et al.*, 2010] and oceanic acidification [*Feely et al.*, 2008]. Studies [*McGregor et al.*, 2007; *Narayan et al.*, 2010; *Gutiérrez et al.*, 2011] in eastern boundary upwelling system (EBUS) regions generally reveal a strengthening trend in upwelling intensity in response to global warming. However, little is known about the behavior of western boundary upwelling in the southwest Asian summer monsoon (ASM) region under modern climate change. This is especially important for the already-stressed upwelling ecosystem in this region due to overfishing, pollution, and growing demand for seafood (e.g., countries in East and South Asia) [*FAO*, 2011].

[3] The monsoon-induced upwelling is one of the dominant features during summer in the northern South China Sea (NSCS) as demonstrated by satellite observations, cruises data, and modeling results [*Jing et al.*, 2009; *Su and Pohlmann*, 2009] (Figure 1a), which represents one of major western boundary upwelling systems and among the most productive regions in the World Ocean. The southwesterly summer monsoon winds (June to August; see Figure S1 in the Supporting Information) induce profound regional upwelling along the east coast of Hainan Island (Figure 1). Sea surface temperature anomaly (SSTA) in the upwelling zone of NSCS is a sensitive indicator of upwelling intensity thus prevailing wind strength, because lower summer sea surface temperature (SST) directly results from cold upwelled waters [*Jing et al.*, 2009; *Su and Pohlmann*, 2009]. Therefore, the paleo-SST records derived from in situ coral skeletal Sr partitioning in this upwelling zone can ideally be used to provide changes of western boundary upwelling and by extension strength of winds associated with ASM. Here we present a monthly-resolved summer SST record (1876–1996) inferred from coral Sr/Ca variations from a massive *Porites* coral, off the east coast of Hainan to investigate long-term upwelling variability in the NSCS.

2. Methods and Samples

[4] In August 1998, a vertical core (2 m in length and 5 cm in diameter) was drilled from a living massive *Porites lutea* coral

Additional supporting information may be found in the online version of this article.

[1]CAS Key Laboratory of Crust-Mantle Material and Environment, School of Earth and Space Science, University of Science and Technology of China, Hefei, China.
[2]State Key Laboratory of Loess and Quaternary Geology, Institute of Earth Environment, Chinese Academy of Sciences, Xi'an, China.
[3]High-Precision Mass Spectrometry and Environment Change Laboratory (HISPEC), Department of Geosciences, National Taiwan University, Taipei, Taiwan.
[4]CAS Key Laboratory of Geospace Environment, School of Earth and Space Sciences, University of Science and Technology of China, Hefei, Anhui, China.
[5]South China Sea Institute of Oceanology, Chinese Academy of Sciences, Guangzhou, China.
[6]Guangzhou Institute of Geochemistry, Chinese Academy of Sciences, Guangzhou, China.
[7]Department of Geography and Anthropology, Louisiana State University, Louisiana, USA.

Corresponding author: Y. Liu, School of Earth and Space Sciences, University of Science and Technology of China, No.96, JinZhai Rd. Baohe District, Hefei, Anhui, 230026, China. (gee@ustc.edu.cn)

C.-C. Shen, High-Precision Mass Spectrometry and Environment Change Laboratory (HISPEC), Department of Geosciences, National Taiwan University, No. 1, Sec. 4, Roosevelt Rd., Taipei 10617, Taiwan. (river@ntu.edu.tw)

0094-8276/13/10.1002/grl.50381

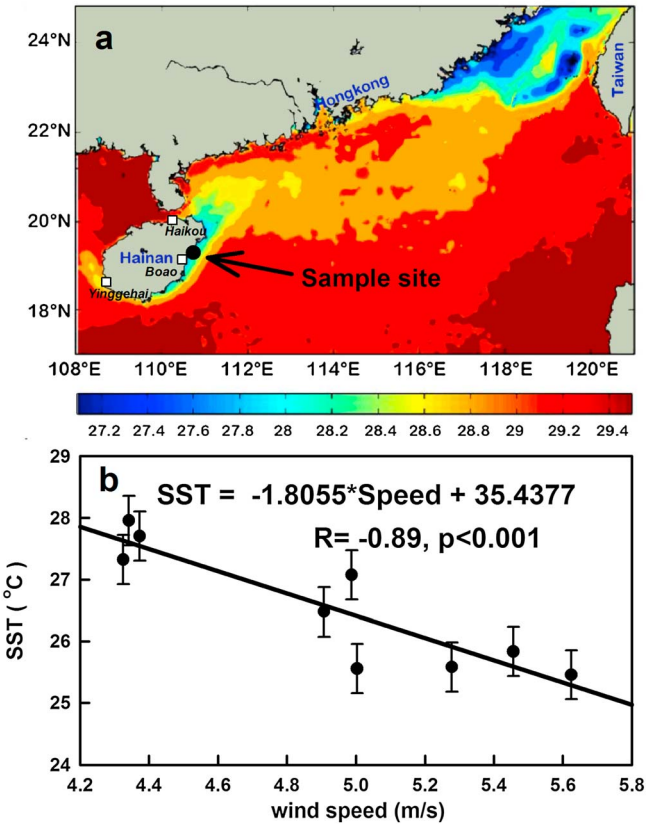

Figure 1. (a) Average summer SST (°C) distributions in the NSCS with data from the Advanced Very High Resolution Radiometer for the interval from 1985–2006, modified from *Jing et al*. [2009]. A comparison with open-ocean SST with the eastern coastal upwelling zone off Hainan reveals a ~1.5°C difference for the location where the core was collected from a live *Porites* coral in 1998. (b) The relationship of coral-inferred summer Boao SST with 1-sigma uncertainty vs. the local satellite wind speed (data from http://podaac.jpl.nasa.gov/) for the interval from 1988–1996.

colony in 5 m of water off Boao in eastern Hainan (19°20′N, 110°39′E) (Figure 1a). Slabs (5 mm thick) were extracted from the cores and washed with ultrapure water then allowed to dry. X-ray images of the slabs reveal annual density bands from 1876–1996 with annual growth rate varying between 10 to 13 mm/yr (Figure S2 of the Supporting Information). X-ray diffraction analysis shows that the coral skeleton is 100% aragonite, and scanning electron microscopy images at core depths of 10, 90, and 180 cm reveals the absence of secondary aragonite. The coral slabs were kept in 10% H_2O_2 for 24 h to decompose organic matter, followed by three rinses with ultrapure water for 5–10 min each. Subsamples (13 per year) were drilled continuously along the maximum growth axis. Coral skeletal Sr/Ca ratios were measured with a Varian Vista inductively coupled plasma atomic emission spectrometer at the Guangzhou Institute of Geochemistry, Chinese Academy of Sciences, following previous techniques [*Schrag*, 1999]. The 1-sigma analytical precision is ±0.20%, corresponding to an SST uncertainty of ±0.39°C.

[5] The 121-year long monthly coral Sr/Ca record reveals seasonal variability with irregular summer values (Figure S3 of the Supporting Information). Age assignment was performed by assigning high coral Sr/Ca value for each seasonal Sr/Ca cycle to a January for each consecutive year (the coldest month based on regional modern instrumental observations [*Yu et al*., 2004]) and then linearly interpolated between these anchor points to monthly intervals. Generally, 3–4 subsamples per year are included in the June-August Sr/Ca data. The derived SST record was calculated with a *Porites* coral Sr/Ca thermometer [SST (°C) = −19.83 × Sr/Ca (mmol/mol) × 10^3 + 210.2 (r = 0.75, n = 147)], calibrated with instrumental SST from a near site at Sanya (18°12′N, 109°29′E), southern Hainan [*Wei et al*., 2000].

[6] The local summer surface wind speed (1988–1996) was calculated as the spatially averaged (110.50°E–111.25°E, 18.75°N–19.50°N) and temporally averaged (from June to August) satellite data obtained from the cross-calibrated multiplatform data set with 0.25° × 0.25° resolution [*Atlas et al*., 2011].

3. Results

[7] The calculated mean summer (June-August) SST data are listed in Table S1 of the Supporting Information. A direct comparison of the coral-derived SST with instrumental data is difficult because there are no long-term in situ data available and gridded data sets (1–2° grid area) smooth out the upwelled cold water SST signal. The absolute summer Sr/Ca SST values in the late 20th century are consistent with the range of SSTs reported by on-site research cruises in the eastern Hainan coast [*Su and Pohlmann*, 2009]. The interdecadal SST mean at Boao is significantly lower than those at nearby sites. For example, the SST mean for Boao is 26.4°C (1960–1996), which is 3–4°C lower than those at the nonupwelling sites [*Yu et al*., 2004], such as Yingehai (30.0°C) and Haikou (30.3°C) at western and northern Hainan for this same time interval (Figure 1a). The low mean summer SST at Boao confirms the strong thermal influence of cold upwelling at this site.

[8] Our reconstructed summer SSTs are significantly negatively correlated with local satellite wind speed (R = −0.89, p < 0.001; Figure 1b), which is consistent with previous studies showing that SST in the upwelling zone of eastern Hainan is dominantly controlled by prevailing wind strength and upwelling intensity [*Jing et al*., 2009; *Su and Pohlmann*, 2009].

4. Discussion and Conclusions

[9] The coral Sr/Ca-derived summer SSTA displays interannual-to-multidecadal variability with anomalies determined as differences from the average of the entire summer SST record (1876–1996; Figure 2). This 121-year sequence can be divided into three periods: Period I (1876–1930) with a higher average summer SSTA of 0.31 ±0.15°C (1 standard deviation of the mean, σ_m), Period II (1931–1960) with a lower average SSTA of −0.75 ±0.16°C (1σ_m), and Period III (1961–1996) featured by an increase to warmer conditions with an average of 0.15 ±0.17°C (1σ_m) (Figure 2).

[10] The changes in summer SSTA noted in our reconstruction is an integrated outcome from the combined effects of cold water upwelling and surface heating. However, the latter effect is considered to be inferior in active upwelling zones [*García-Reyes and Largier*, 2010]. The long-term Boao summer SSTA time series is not characterized with a

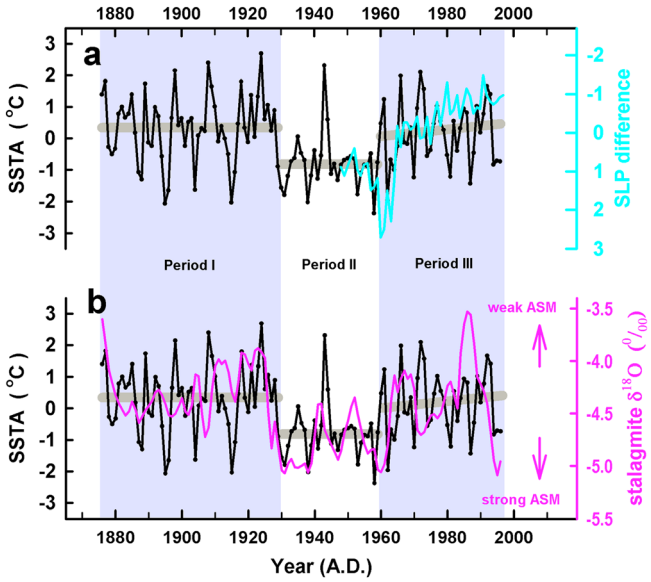

Figure 2. Time series of (a) summer Boao SSTA (black) in the upwelling zone of NSCS with the normalized mean latitudinal differences (blue) of sea level pressure between 10°N and 50°N within 110°E–160°E [*Jiang and Wang*, 2005], and (b) Indian stalagmite $\delta^{18}O$ (pink) [*Sinha et al.*, 2011], representing ASM intensity (arrows). The summer SSTA are calculated relative to the mean of summer SST for entire time series. The thick gray lines indicate the linear trend of SSTA during each period. Note that the axis of sea level pressure is plotted with a reverse axis. Oxygen isotope ratios are expressed in δ notation relative to the Vienna Pee-Dee Belemnite standard.

global warming-like monotonous trend [*Jones et al.*, 1999]. Northern Hemisphere temperature increased by 0.6 ± 0.1°C ($1\sigma_m$) from 1920 to 1990 [*Jones et al.*, 1999] (Figure S4 of the Supporting Information). In the central South China Sea (SCS), a region with no upwelling, a coral-based reconstruction reveals there are stable SST with a year-to-year fluctuation of ± 0.8°C ($1\sigma_m$) for 1900–1930 with a 2.1°C warming trend from 1930 to 1990 [*Sun et al.*, 2004] (Figure S4 of the Supporting Information). This SST increase is not present in the Boao record and this record contains transitions in 1930–1931 and 1960–1961 (Figure 2). Moreover, there is an insignificant correlation coefficient between Boao SSTA and Northern Hemisphere temperature anomaly since 1950 ($R = 0.19$, $p = 0.254$) suggesting a weak influence of global warming for this upwelling region.

[11] Multidecadal variability in the Boao summer SSTA reconstruction is consistent with the instrumental monsoon index [*Jiang and Wang*, 2005] (Figure 2a), and Indian stalagmite inferred ASM intensity [*Sinha et al.*, 2011] (Figure 2b). The stalagmite $\delta^{18}O$ records from the core of the monsoon region in India has been shown to reflect changes of summer monsoon precipitation or ASM intensity; with more negative stalagmite $\delta^{18}O$ values indicating stronger ASM intensity and vice versa [*Sinha et al.*, 2011]. Around 1960, both the land-sea pressure gradient and summer rainfall records show a similar step-like shift. Another SSTA shift between Period I and II of our reconstruction corresponds to a similar shift in the Indian speleothem $\delta^{18}O$ record. Boao summer SSTA is significantly correlated with Indian speleothem $\delta^{18}O$ ($R = 0.32$ and 0.69, for raw and 7 year moving-average respectively, for 1876–1996; $p < 0.001$). Clearly, large-scale monsoon circulation dominates the Boao summer SSTA time series on multidecadal time scales. Strong ASM enhances regional upwelling, resulting in a zonal cooling offshore of Boao. Accordingly, the Boao summer SSTA can be considered as an upwelling proxy that reflects ASM intensity with low summer SSTA caused by strong upwelling, and vice-versa.

[12] Current findings for coastal upwelling dynamics in response to climate change are mainly from the EBUSs where along-shore and equatorward winds drive surface Ekman transport offshore. High-resolution marine sediment records [*McGregor et al.*, 2007; *Gutiérrez et al.*, 2011] and observation data [*Narayan et al.*, 2010] show an enhanced upwelling intensity for the most recent 50 years in the EBUSs in response to a strengthening of upwelling-favorable winds, which are attributed to the intensification of the land-sea pressure gradient due to global warming [*McGregor et al.*, 2007; *Bakun et al.*, 2010] (Figure 3). Both the Peru and Africa coastal upwelling systems show a decreasing trend SSTA from 1960 to 2000, which is inferred as increased upwelling (Figure 3). However, the NSCS reconstruction shows a step-like shift to higher SSTA thus a decline in upwelling from 1960 to 1996 (Figure 3). Similar trends have been reported

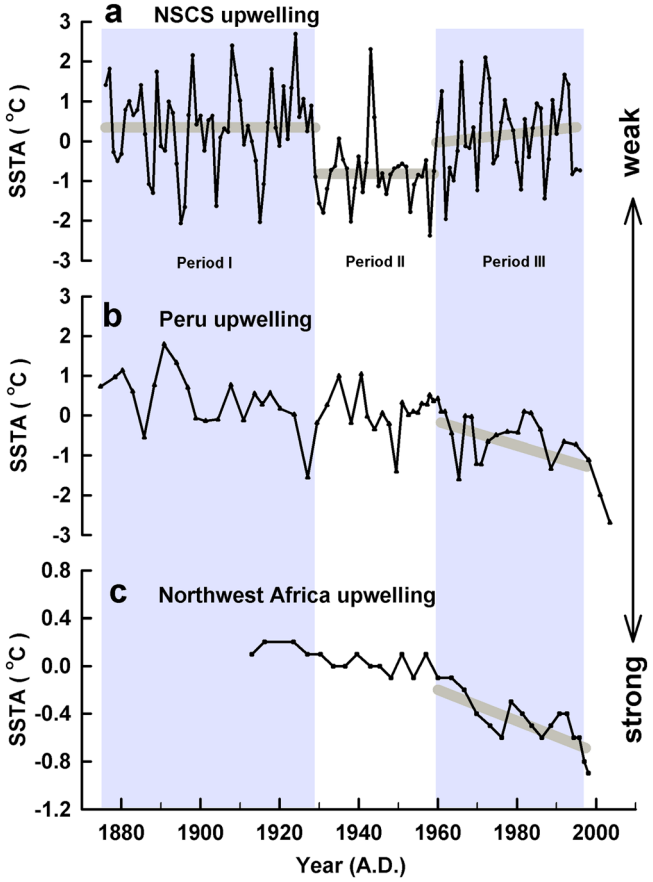

Figure 3. Time series of SSTA in the upwelling zones of (a) NSCS, (b) Peru [*Gutiérrez et al.*, 2011], and (c) Northwest Africa [*McGregor et al.*, 2007]. Note there is significant SSTA trend difference in the late-20th century between Boao and the two EBUS sites (thick gray lines).

in other Asia monsoon areas, including a weakening surface wind speed [*Xu*, *et al*., 2006], and increasing drought events with declining precipitation over South Asia and northern China [*Ramanathan and Carmichael*, 2008].

[13] The proxy-inferred evidence and instrumental records indicate a decrease in the strength of the ASM from 1960 to 1996 (Figure 2). One possible mechanism for the weakening ASM is the so-called "sunlight dimming" process [*Ramanathan and Carmichael*, 2008]. Anthropogenic air pollution, including black carbon, sulfate, nitrate, and fly ash, released from fossil fuel combustion and biomass burning in Asia, related to economic development in recent decades, has resulted in dimming and surface cooling [*Ramanathan and Carmichael*, 2008]. These lingering anthropogenic aerosols can reduce the amount of solar radiation reaching the surface by as much as 20 Wm^{-2}, likely resulting in a weakening of monsoonal circulation and near surface wind speed [*Ramanathan and Carmichael*, 2008]. We suggest that air pollution, which cools land surfaces, has reduced the monsoon-induced western boundary upwelling along coastal south Asia, whereas high atmospheric greenhouse gas content, which warms land surfaces, is strengthening EBUS.

[14] The large interannual-to-multidecadal variability of monsoon-induced regional upwelling revealed here offers an essential reference to evaluate the global-climate impact on fisheries in this monsoonal upwelling region in the near future. This is of particular importance because the NSCS with its high biodiversity constitutes one of the most productive ecosystems in the world [*Sumaila et al*., 2011]. Whereas coastal upwelling brings nutrient-rich deep cold water, it also carries CO_2-rich and acidic water into the surface. With the addition of anthropogenic CO_2 emissions that are acidifying the surface oceans [*Caldeira and Wickett*, 2003], this is a serious threat to marine calcifying organisms in upwelling regions. Acidification not only affects calcification rates for marine organisms [*Orr et al*., 2005], but it also damages the nervous systems of fish [*Nilsson et al*., 2012]. Observations clearly show that increased upwelling of the CO_2-rich and corrosive deep water in eastern boundary current regions has enhanced the advancement of low pH seawater into broad regions of the western continental shelf of North American [*Feely et al*., 2008]. Conversely, the decreasing trend in late the 20th-century of summer upwelling in the NSCS, associated with western boundary upwelling systems (Figure 3), thus a reduction in upwelling of CO_2-rich seawaters, could be critical for the sustainability of this regional marine ecosystem in the face of global ocean acidification, especially for the valuable and abundant coral reefs in this region.

[15] **Acknowledgments.** This research was supported by the National Key Basic Research Program of China (2013CB956102), the Strategic Priority Research Program, CAS (XDA05080301), National Science Foundation of China (40830852,41003002 and 41262001), State Key Laboratory of Loess and Quaternary Geology, Institute of Earth Environment, CAS (SKLLQG1205), State Key Laboratory of Isotope Geochemistry, Guangzhou Institute of Geochemistry, CAS(GIGiso-12-01,-12-02) and Taiwan ROC NSC (99-2811-M-002-184 and 99-2611-M-002-005) and National Taiwan University (101R7625 and 102R7625).

References

Atlas, R., R. N. Hoffman, J. Ardizzone, S. M. Leidner, J. C. Jusem, D. K. Smith, and D. Gombos (2011), A cross-calibrated, multiplatform ocean surface wind velocity product for meteorological and oceanographic applications, *Bull. Amer. Meteor. Soc.*, *92*, 157–174, doi:10.1175/2010BAMS2946.1.

Bakun, A., D. B. Field, A. Redondo-Rodriguez, and S. J. Weaks (2010), Greenhouse gas, upwelling-favorable winds, and the future of coastal ocean upwelling ecosystems, *Glob.ChangeBiol.*, *16*, 1213–1228, doi:10.1111/j.1365-2486.2009.02094.X.

Caldeira, K., and M. E. Wickett (2003), Anthropogenic carbon andocean pH, *Nature*, *425*, 365, doi:10.1038/425365a.

Feely, R. A., C. L. Sabine, J. M. Hernandez-Ayon, D. Ianson, and B. Hales (2008), Evidence for Upwelling of Corrosive "Acidified" Water onto the Continental Shelf, *Science*, *320*, 1490–1492, doi:10.1126/science.1155676.

Food and Agriculture Organization (2011), *The State of World Fisheries and Aquaculture 2010*, FAO, Rome.

García-Reyes, M., and J. Largier (2010), Observations of increased wind-driven coastal upwelling off central California, *J. Geophys. Res.*, *115*, C04011, doi:10.1029/2009JC005576.

Gutiérrez, D., et al. (2011), Coastal cooling and increased productivity in the main upwelling zone off Peru since the mid-twentieth century, *Geophys. Res. Lett.*, *38*, L07603, doi:10.1029/2010GL046324.

Jiang, D., and H. Wang (2005), Natural interdecadal weakening of East Asian summer in the late 20th century, *Chinese Sci. Bull.*, *50*, 1923–1929, doi:10.1360/982005-36.

Jing, Z., Y. Qi, Z. Hua, and H. Zhang (2009), Numerical study on the summer upwelling system in the northern continental shelf of the South China Sea, *Cont. Shelf Res.*, *29*, 467–478, doi:10.1016/j.csr.2008.11.008.

Jones, P. D., M. New, D. E. Parker, S. Martin, and I. G. Rigor (1999), Surface air temperature and its changes over the past 150 years, *Rev. Geophys.*, *37*, 173–199, doi:10.1029/1999RG900002.

McGregor, H. V., M. Dima, H. W. Fischer, and S. Mulitza (2007), Rapid 20th-century increase in coastal upwelling off northwest Africa, *Science*, *315*, 637–639, doi:10.1126/science.1134839.

Narayan, N., A. Paul, S. Mulitza, and M. Schulz (2010), Trends in coastal upwelling intensity during the late 20th century, *Ocean Sci.*, *6*, 815–823, doi:10.5194/os-6-815-2010.

Nilsson, G. E., D. L. Dixson, P. Domenici, M. I. McCormick, C. Sørensen, S. Watson, and P. L. Munday (2012), Near-future carbon dioxide levels alter fish behaviour by interfering with neurotransmitter function, *Nat. Clim. Change*, *2*, 201–204, doi:10.1038/nclimate1352.

Orr, J. C., et al. (2005), Anthropogenic ocean acidification over the twenty-first century and its impact on calcifying organisms, *Nature*, *437*, 681–686, doi:10.1038/nature04095.

Ramanathan, V., and G. Carmichael (2008), Global and regional climate changes due to black carbon, *Nat. Geosci.*, *1*, 221–227, doi:10.1038/ngeo156.

Schrag, D. P. (1999), Rapid analysis of high-precision Sr/Ca ratios in corals and other marine carbonates, *Paleoceanography*, *14*, 97–102, doi:10.1029/1998PA900025.

Sinha, A., M. Berkelhammer, L. Stott, M. Mudelsee, H. Chen, and J. Biswas (2011), The leading mode of Indian Summer Monsoon precipitation variability during the last millennium, *Geophys. Res. Lett.*, *38*, L15703, doi:10.1029/2011GL047713.

Su, J., and T. Pohlmann (2009), Wind and topography influence on an upwelling system at the eastern Hainan coast, *J. Geophys. Res.*, *114*, C06017, doi:10.1029/2008JC005018.

Sumaila, U. R., W. W. L. Cheung, V. W. Y. Lam, D. Pauly, and S. Herrick (2011), Climate change impacts on the biophysics and economics of world fisheries, *Nat. Clim. Change*, *1*, 449–346, doi:10.1038/nclimate1301.

Summerhayes C.P. (1996), *Ocean Resources in Oceanography*: *an Illustrated Guide*, edited by C.P. Summerhayes, and S.A. Thorpe, pp. 314–337, Manson Publishing, London.

Sun, Y., M. Sun, G. Wei, T. Lee, B. Nie, and Z. Yu (2004), Strontium contents of a Porites coral from Xisha Island, South China Sea: A proxy for sea-surface temperature of the 20th century, *Paleoceanography*, *19*, PA2004, doi:10.1029/2003PA000959.

Wang, M., J. E. Overland, and N. A. Bond (2010), Climate projections for selected large marine ecosystems, *J. Marine Syst.*, *79*, 258–266, doi:10.1016/j.jmarsys.2008.11.028.

Wei, G., M. Sun, X. Li, and B. Nie (2000), Mg/Ca, Sr/Ca and U/Ca ratios of a Porites coral from Sanya Bay, Hainan Island, South China Sea and their relationships to sea surface temperature, *Palaeogeogr. Palaeoclimatol. Palaeoecol.*, *162*, 59–74, doi:10.1016/S0031-0182(00)00105-X.

Xu, M., C. Chang, C. Fu, Y. Qi, A. Robock, D. Robinson, and H. Zhang (2006), Steady decline of East Asian monsoon winds, 1961–2000: Evidence from direct measurements of wind speed, *J. Geophys. Res.*, *111*, D24111, doi: 10.1029/2006JD007337.

Yu, K., J. Zhao, T. Liu, G. Wei, P. Wang, and K. D. Collerson (2004), High-frequency winter cooling and reef coral mortality during the Holocene climatic optimum, *Earth Planet. Sci. Lett.*, *224*, 143–155, doi:10.1016/j.epsl.2004.04.036.